Deep Learning-Based Crack Detection on Complex Decorative Surfaces of Cultural Heritage Artifacts

HongYi Shih[1(✉)], Debora Verniz[1], Filiz Bunyak[2], and Jessica Boldt[3]

[1] Department of Architectural Studies, University of Missouri, Columbia, USA
{hsgg6,vernizd}@missouri.edu
[2] Department of Electrical Engineering and Computer Science, University of Missouri, Columbia, USA
bunyak@missouri.edu
[3] Museum of Anthropology, University of Missouri, Columbia, USA
boldtj@missouri.edu

Abstract. Artifact condition monitoring plays an important role in heritage preservation, as surface deterioration may lead to irreversible damage. However, detecting fine cracks on decorative artifacts is particularly challenging due to the presence of complex surface patterns that can obscure crack features. In this study, we develop a deep learning-based approach for crack detection on texture-rich cultural heritage artifacts. A dataset of 481 images was collected from four hand-painted terracotta lids, including both cracked and intact samples. We trained a YOLOv8 segmentation model and evaluated its performance under different experimental settings. Specifically, we investigated the effects of several preprocessing strategies, including background removal, specular reflection mitigation, and contrast enhancement, as well as the influence of dataset size, input resolution, and transfer learning. Our results show that reducing visual interference leads to more reliable detection, while increasing the dataset size improves model stability and generalization. We also observed that contrast enhancement changes the visibility of cracks under complex surface conditions but does not consistently improve overall performance. In addition, transfer learning from an infrastructure crack dataset increases precision in some cases, but can reduce recall, likely due to domain differences. Despite these improvements, the model still struggles with highly patterned surfaces, indicating the inherent difficulty of crack detection in decorative artifacts. These findings highlight key factors that affect model performance and provide practical insights for applying deep learning methods in digital heritage preservation.

Keywords: Deep Learning · Cultural Heritage · Crack Detection · Image Processing · Digital Preservation

© The Author(s), under exclusive license to Springer Nature Switzerland AG 2027
O. Gervasi et al. (Eds.): ICCSA 2026, LNCS 16767, pp. 478–491, 2027.
https://doi.org/10.1007/978-3-032-30491-9_30

1 Introduction

Cultural heritage condition monitoring is essential for preservation, as ongoing deterioration can lead to irreversible damage. Early detection and intervention help mitigate further degradation and support long-term conservation. However, traditional condition assessment relies on visual inspection, which is time-consuming and often lacks consistency [1]. Among various forms of deterioration, cracks are one of the most common and critical types, as they directly reflect structural vulnerability and ongoing material degradation. If there is no timely intervention, cracks may propagate and result in more severe damages [2]. However, the fine and irregular features of cracks make detection particularly challenging [3].

These challenges highlight the need for automated and objective detection approaches in heritage preservation. For this purpose, many applications have emerged in recent years and among those, computer vision techniques provide automated, non-invasive approaches for deterioration detection [4], whereas convolutional neural network (CNN)–based deep learning models have become powerful tools for deterioration detection and demonstrated promising performance. For instance, on crack detection tasks, Yiğit and Uysal [5] achieved approximately 83% accuracy in heritage structural inspection. Similarly, Huang et al. [6] developed a two-stage deep learning framework, achieving approximately 3% crack length estimation error.

However, despite these promising results, condition assessment tasks become more challenging when complex decorative patterns are present [7]. This challenge is especially pronounced in cultural heritage artifacts, which often exhibit rich surface decorations that may visually resemble crack-like structures, introducing significant interference for automated detection [8]. Despite this challenge, limited research has systematically analyzed the impact of different factors on crack detection performance in such complex conditions.

This study investigates and evaluates key factors influencing crack detection performance on cultural heritage artifacts with complex decorative surfaces through ablation experiments. A dataset was constructed using artifacts from the Museum of Anthropology, University of Missouri as a case study. Key factors were identified through literature review and were systematically evaluated. Finally, this study provides insights into improving detection performance and outlines directions for future research.

2 Literature Review

This literature review synthesizes key factors in deep learning-based detection tasks and examines how they may affect crack detection under complex surface conditions.

Various sources of visual interference can degrade model performance in detection tasks. For instance, complex backgrounds can introduce irrelevant patterns that lead to false positives and feature confusion [9], making it more difficult to separate target objects from surrounding regions.

Beyond background complexity, variability in lighting conditions can significantly affect crack visibility, as changes in illumination may introduce misleading patterns that

resemble cracks, making detection more challenging [10]. In addition, specular reflections can produce strong highlights and distortions that complicate image interpretation and degrade the performance of detection tasks [11].

Another related factor is the contrast between cracks and their surrounding background material. For example, in pavement crack detection, background texture can interfere with the continuity of cracks and reduce their distinguishability [12]. Similar to concrete, material degradation reduces the contrast between cracks and the background, thereby impairing detection performance [13].

The above-mentioned factors make image preprocessing critical in detection pipelines that enhances relevant visual features and suppresses noise, thereby directly influencing the performance of deep learning models [14, 15].

In addition to image-level factors, data representation also plays a crucial role. In object detection tasks, higher-resolution inputs can improve the representation of small or subtle features, whereas lower resolutions may result in the loss of critical details [16].

Furthermore, transfer learning has been shown to improve model generalization. Zhang et al. [17] demonstrated that low-level features such as edges and textures can be effectively transferred to pavement crack detection tasks using transfer learning, improving the model's ability to distinguish cracks from complex background patterns. Suryawanshi et al. [18] further applied transfer learning to crack detection in ancient wall paintings, but highlighted challenges caused by visually similar features such as brush strokes and textures. These findings suggest that, despite its advantages, transfer learning may still be ineffective in scenarios with complex surface patterns.

Taken together, these studies highlight several factors that may influence crack detection performance under complex surface conditions, including background complexity, lighting conditions, specular reflections, contrast, input resolution, and transfer learning.

3 Methodology

This study has five main steps: data collection, image processing, annotation and dataset split, model training, and evaluation. The proposed pipeline is shown in Fig. 1.

3.1 Data Collection

490 images of four hand-painted terracotta lids (Fig. 2) were collected over three sessions. Images were captured using a turntable from multiple viewing angles, including both the front and reverse surfaces of each lid, under consistent lighting conditions. Three lids contained visible cracks (Fig. 2a-c), while one intact lid was included as a negative sample (Fig. 2d). After removing duplicate and blurred images, 481 images were retained.

3.2 Image Processing

To reduce visual interference and enhance crack visibility, several image preprocessing strategies were investigated in the ablation experiments. These strategies can be

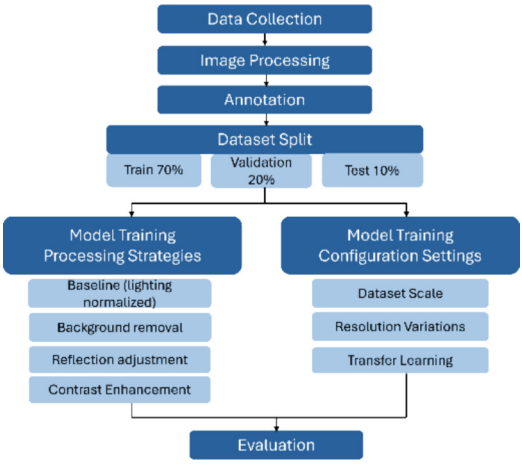

Fig. 1. Proposed crack detection workflow for artifacts with decorative patterns.

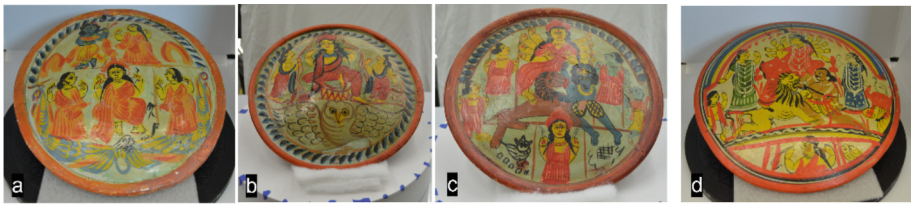

Fig. 2. (a–c) Three cracked samples. (d) One intact sample.

conceptually categorized into two groups: (1) interference reduction, including lighting normalization, background removal, and specular reflection mitigation to minimize noise; and (2) crack feature enhancement, including contrast enhancement and resolution adjustment. Lighting normalization was first applied to reduce illumination variability across acquisition rounds. Background removal was performed using a YOLOv8-based approach to localize the pottery lid region and isolate the artifacts from the background (Fig. 3b). Specular regions were identified based on intensity threshold and subsequently reconstructed using inpainting techniques (Fig. 3c). For crack feature enhancement, contrast enhancement was applied to improve crack visibility while minimizing texture amplification (Fig. 3d), whereas resolution adjustment was used to preserve fine structural details of cracks.



Fig. 3. (a) Raw image. (b) Background removed. (c) Specular reflection adjusted (before and after). (d) Contrast enhanced (before and after).

3.3 Crack Annotation

For the annotation process, Roboflow [19] was used to annotate cracks using the polygon tool. In this project, cracks were operationally defined as thin, elongated linear features exhibiting depth cues, such as subtle shadowing along the fractured path. Due to the difficulty of detecting fine linear cracks with deep learning models, annotated regions were slightly expanded to include surrounding context and improve model learning. The annotated dataset was split into 70% for training, 20% for validation, and 10% for testing.

3.4 Model Training

YOLOv8n model [20] was used for training for its efficiency and suitability for small datasets. A series of controlled experiments were designed to evaluate the impact of different processing strategies and training configurations on crack detection performance. A baseline model was first trained using images with lighting normalization applied to ensure consistent illumination. This was followed by a systematic evaluation of different preprocessing strategies.

The best-performing preprocessing configuration was then selected as the reference condition. Based on this configuration, further experiments were conducted to investigate the effects of dataset scale, input resolution, and transfer learning on model performance. Dataset scale refers to increasing the number of training images under the same preprocessing pipeline to evaluate the effect of training data size. For resolution analysis, the input size was increased from 640 × 640 to 1024 × 1024 to examine its impact on detecting fine crack structures. For transfer learning, a crack segmentation model pretrained on an infrastructure crack dataset [21] was fine-tuned on the terracotta crack dataset to evaluate cross-domain knowledge transfer. The configurations are summarized in Table 1.

Table 1. Summary of ablation experiments.

Configuration	Description
Baseline	200 images with lighting normalization applied.
Background and Reflection	200 images with background removal and reflection adjustment applied.
Dataset Scale	Expanded from 200 to 481 images, with background removal and reflection adjustment applied.
Contrast Enhancement	481 images with background removal, reflection adjustment, and contrast enhancement applied.
Resolution	Input resolution increased from 640 × 640 to 1024 × 1024, with background removal and reflection adjustment applied.
Transfer Learning	A pretrained crack segmentation model (infrastructure dataset) fine-tuned on terracotta images, with background removal and reflection adjustment applied.

(*continued*)

Table 1. (*continued*)

Configuration	Description
Note: Lighting normalization was applied in all configurations. All experiments used an input resolution of 640 × 640, except the resolution test (1024 × 1024).	

3.5 Evaluation

Model performance was evaluated using three approaches: (1) quantitative metrics, including precision, recall, and mean Average Precision at 0.5 Intersection over Union (mAP@0.5); (2) qualitative visualization of detection results, and (3) external images to assess generalization to unseen data. These evaluations were used to identify factors contributing to variations in model performance.

4 Results

4.1 Quantitative Evaluation on the Internal Dataset

The quantitative results of the six ablations are compared, including precision, recall, and mAP@0.5. Precision and recall follow Eqs. (1) and (2).

$$\text{Precision} = \frac{TP}{TP + FP} \tag{1}$$

$$\text{Recall} = \frac{TP}{TP + FN} \tag{2}$$

True Positive (TP) represents correctly detected crack instances, False Positive (FP) corresponds to background regions incorrectly identified as cracks, and False Negative (FN) denotes crack instances that are not detected and are instead classified as background.

The mAP@0.5 metric evaluates detection performance by computing the area under the precision–recall curve at an Intersection over Union (IoU) threshold of 0.5. Predictions with IoU $\geq$ 0.5 are considered correct. The IoU is defined in Eq. (3).

$$\text{IoU} = \frac{\text{Area of Overlap}}{\text{Area of Union}} \tag{3}$$

The quantitative outcomes of precision, recall, and mAP@0.5 are presented in Table 2. These metrics provide a comprehensive evaluation of detection performance, reflecting the trade-off between precision (false positives), recall (missed detections), and overall localization accuracy (mAP).

Table 2. Quantitative results of ablation experiments.

	Precision	Recall	mAP@0.5
Baseline	0.051	0.046	0.008
Background and reflection	0.138	0.074	0.050
Dataset expansion	0.615	0.408	0.4
Contrast enhancement	0.608	0.369	0.393
Resolution	0.573	0.464	0.461
Transfer learning	0.634	0.458	0.483

The precision-recall (PR) curves in Fig. 4 illustrate the trade-off between precision and recall across all ablation settings. These curves provide an assessment of detection performance across different configurations.

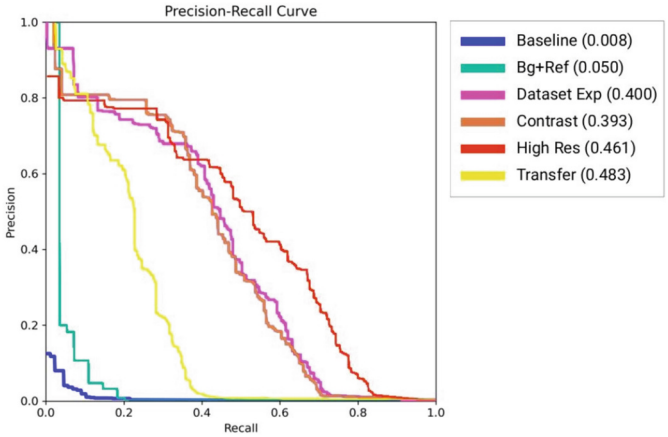

Fig. 4. Precision–recall curves for different configurations.

4.2 Qualitative Evaluation on the Internal Dataset

The qualitative results, including ground truth and detection outputs for the six ablation settings, are presented in Table 3 for comparison. These visual illustrations support quantitative findings and reveal detection behaviors.

Table 3. Qualitative comparison of crack detection results.

	Ground Truth	Crack detection results
Baseline	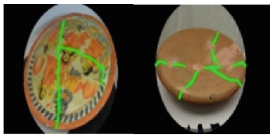	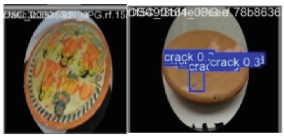
Background and reflection	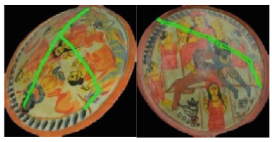	
Dataset expansion	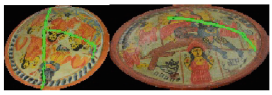	
Contrast enhancement		
Resolution	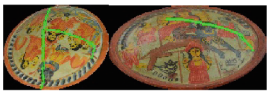	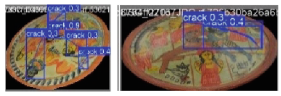
Transfer learning	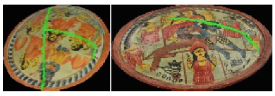	

For the baseline model, few cracks are detected. With precision, recall, and mAP@0.5 all close to zero (0.051, 0.046, and 0.008 respectively), the model exhibits limited ability to learn discriminative features and is unable to distinguish among different visual interferences (specular reflections, cluttered backgrounds, and decorative patterns). The blue PR curve demonstrates that the performance remains close to the origin, reflecting consistent low precision and recall across different confidence thresholds. This deficiency is further explained by the visual results, where cracks are only detected on plain-pattern surfaces (e.g., the reverse side of the artifact), while detection fails on surfaces with complex decorative patterns. These results suggest that the model is highly sensitive to surface complexity and visual noise.

After applying background removal and reflection mitigation, the detection performance improves evidently. Precision, recall, and mAP@0.5 increase from 0.051 to 0.138 (+170.6%), 0.046 to 0.074 (+60.9%), and 0.008 to 0.050 (+525%), respectively. The PR curve (green line) moves slightly away from the origin, indicating a more stable detection behavior across confidence thresholds. The visualized results show that reducing background noise and specular reflections improves the model ‘s ability to localize crack

regions. However, the model still shows difficulty distinguishing cracks from decorative patterns, often producing fragmented or incomplete detections.

After validating the effectiveness of background and reflection removal, the dataset was expanded from 200 to 481 images to enhance data diversity and to improve detection performance. The model shows the detection performance improves substantially. Precision increases from 0.138 to 0.615 (+345.6%), recall from 0.074 to 0.408 (+451.3%), and mAP@0.5 from 0.050 to 0.400 (+700%). The PR curve (pink line) further indicates the performance improves across a wider range of confidence thresholds. The visualized results further depict this improvement. More crack regions are detected, and cracks appear more continuous and better aligned with ground truth annotations. However, missed detections still occur with dataset expansion.

Following dataset expansion and prior preprocessing, contrast enhancement was additionally applied. With contrast enhancement, precision slightly decreases from 0.615 to 0.608 (−1.1%), recall from 0.408 to 0.369 (−9.6%), and mAP@0.5 from 0.400 to 0.393 (−1.8%). The PR curve (orange line) remains similar to the dataset expansion model, indicating improvement in overall detection performance is limited. Qualitative results show some additional local responses in crack-like regions; however, the detections appear to be more fragmented and do not translate to better overall quantitative performance.

Since contrast enhancement did not improve performance, higher resolution (1024 × 1024) was applied based on the dataset expansion setting. With higher resolution, mAP@0.5 increases from 0.400 to 0.461 (+15.3%), and recall improves from 0.408 to 0.464 (+13.7%), while precision slightly decreases from 0.615 to 0.573 (−6.8%). The PR curve (red line) shifts further from the origin, particularly in the higher recall region, indicating detection coverage is improved. Qualitative results show that higher resolution enables better detection of fine crack details and more complete crack structures. However, higher resolution also introduces additional false positives, particularly in highly textured regions, that reveals a trade-off between recall and precision.

Based on the dataset expansion setting, transfer learning was applied using a pretrained infrastructure crack detection model. The transfer learning model achieves the highest precision (0.634) and mAP@0.5 (0.483), while recall (0.458) remains slightly lower than the higher resolution model. However, the PR curve (yellow line) sharply drops beyond the low-recall region, indicating that its performance is concentrated within a limited range of high-confidence detections rather than being sustained across the full recall range. Qualitative results further reveal that detection coverage is limited. Although some crack regions are detected with high confidence and appear to be less fragmented, other crack regions remain entirely undetected.

4.3 External Evaluation

For the external evaluation, artifacts with different shapes and levels of decorative complexity were selected to assess the model's generalization to unseen data. The first artifact is a cup with a plain surface and both thick and thin cracks (Fig. 5a). The second artifact is a fruit stand with regular geometric decorations on the surface (Fig. 5b). The third artifact is a kymbe (shallow vessel) with complex painted patterns and fine cracks (Fig. 5c).



Fig. 5. External pottery artifacts: (a) a cup with a plain surface, (b) a fruit stand with geometric decoration, and (c) a kymbe with complex painted patterns. Adapted from [22–24].

The transfer learning model which achieves the best performance (Table 2) was selected to detect the cracks in the external images. The results are qualitatively and quantitatively presented simultaneously for clear review. Visual comparisons between the ground truth and the detection results are provided, along with quantitative metrics of precision and recall, as shown in Table 4.

Table 4. Crack detection results on external artifacts.

Artifact	Ground Truth	Crack detection results	Precision	Recall
Cup	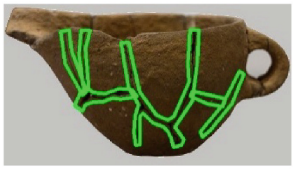	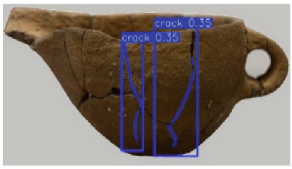	0.932	0.167
Fruit stand			0.927	0.412
Kymbe			0.983	0.080

Among the three sample artifacts, precision is always high (ranging from 0.927 to 0.983), where recall varies but remains low overall (between 0.080 and 0.412). For the cup artifact, the model detects several main cracks, but is unable to detect the thicker cracks, resulting in low recall (0.167) despite high precision (0.932). For the fruit stand artifact, the model is able to distinguish cracks from the geometric patterns with some cracks missing, leading to moderate recall (0.412) and high precision (0.927). For the kymbe artifact, the model fails to distinguish cracks from the complex patterns with only one crack detected. As a result, precision remains high (0.983), while recall is extremely low (0.080).

5 Discussion

5.1 Internal Evaluation

This study examines how different preprocessing strategies and model configurations may affect crack detection performance on artifacts with complex decorative patterns. The results reveal that detection performance is strongly influenced by surface texture and visual interference, and that different strategies introduce clear trade-offs between precision and recall. Based on the above stated observations, several key insights can be drawn as core emphasis.

First, reducing visual interference through background removal and specular reflection mitigation improves detection performance. Those factors often introduce patterns that resemble cracks, particularly on textured artifact surfaces. While this preprocessing leads to noticeable improvement compared to the baseline, it is not sufficient to fully address the challenges introduced by complex decorative patterns.

Second, dataset expansion plays an important role in improving detection performance. Increasing both the number and diversity of training images leads to consistent improvements across precision, recall, and mAP@0.5. This behavior suggests that representative in-domain data is more critical than preprocessing alone for supporting generalization on complex surfaces.

Third, visual enhancement strategies do not always lead to better results on texture-rich artifacts. Although both contrast enhancement and higher resolution increase the visibility of fine details, their effects differ and somewhat contradictive. Contrast enhancement tends to amplify surface texture and noise, which often results in more fragmented detections but not improving overall performance. In contrast, higher resolution improves recall and mAP@0.5 by preserving finer crack details but slightly reduces precision due to an increase in false positives.

Finally, transfer learning appears to be domain sensitive. Although the pretrained infrastructure crack model achieves the highest precision and mAP@0.5, its performance is concentrated in a limited high-confidence region and does not remain stable across the full recall range. Qualitative results also show incomplete crack coverage, suggesting that domain differences between infrastructure surfaces and decorated artifact surfaces restrain effective knowledge transfer.

5.2 External Evaluation

The external evaluation reveals the strengths and limitations of the model's ability to detect cracks across different levels of pattern complexity and crack types. The high precision and low recall scenario indicate accurate detection but a missing of large portion of cracks. This is likely due to visual interference and dataset bias.

First, detection performance is strongly affected by visual interference from surface patterns. This may be related to the structural characteristics of the patterns. The geometric patterns are relatively regular and well-structured, making them easier for the model to distinguish from cracks. In contrast, irregular and densely distributed patterns introduce greater visual interference and share similar features with cracks, making accurate detection more difficult to achieve.

Second, the training data is dominated by thin cracks, leading the model to be biased toward thin crack features and limiting its ability to detect thicker cracks.

It should be noted that although artifacts with different shapes were included in the external evaluation, no clear evidence was found to suggest that shape influences detection performance.

Overall, the results suggest that the model exhibits conservative detection behavior. While precision remains consistently high, recall varies across different conditions, indicating condition-dependent generalization.

6 Conclusion

This study shows that crack detection performance on artifacts with complex decorative patterns is strongly influenced by surface texture and visual interference. Different preprocessing strategies and configurations lead to clear trade-offs among precision, recall, and detection coverage, suggesting that no single approach consistently optimizes all aspects of performance. Considering the visual complexity of heritage artifacts, methods developed for conventional computer vision tasks may not transfer appropriately. Instead, the effectiveness of conventional computer vision methods appears to depend on the characteristics of the target surface and the intended detection goals.

Although the results highlight several important factors that affect crack detection, a number of challenges remain. First, while performance improves under different configurations, the overall detection metrics are still moderate, suggesting that further improvement is necessary. Second, the dataset size is relatively small and includes artifacts with similar decorative patterns. This is further reflected in the external evaluation that the generalization performance decreases under complex visual conditions. Third, the annotated cracks are primarily subtle and thin, which biases the model toward thin crack features and limits its ability to detect cracks with different scales and characteristics.

Future works will explore models that are better suited for capturing fine, crack-specific features, particularly for subtle and elongated structures. In addition, expanding the dataset to include a wider range of decorative patterns and crack variations is essential for improving generalization across diverse artifact surfaces.

Author Contributions. H. Shih designed and performed the experiments and wrote the manuscript. D. Verniz and F. Bunyak supervised the project and reviewed the final version of the manuscript. F. Bunyak provided guidance on image processing and deep learning methods. H. Shih, D. Verniz, and J. Boldt collected the data.

Acknowledgments. We are grateful to the Museum of Anthropology at the University of Missouri-Columbia for providing access to the collections.

Disclosure of Interests. The authors have no competing interests to declare that are relevant to the content of this article.

References

1. Mishra, M., Lourenço, P.B.: Artificial intelligence-assisted visual inspection for cultural heritage: state-of-the-art review. J. Cult. Herit. **66**, 536–550 (2024). https://doi.org/10.1016/j.culher.2024.01.005

2. Wang, H., Shi, Y., Yuan, Q., Li, M.: Crack detection and feature extraction of heritage buildings via point clouds: a case study of Zhonghua Gate Castle in Nanjing. Buildings. **14**, 2278 (2024). https://doi.org/10.3390/buildings14082278
3. Zhang, Y.: Knowledge of earthen heritage deterioration in dry areas of China: salinity effect on the formation of cracked surface crust. Herit. Sci. **11**, 41 (2023). https://doi.org/10.1186/s40494-023-00890-y
4. Carvalho Ottoni, A.L., Cordeiro Ottoni, L.T.: A deep learning approach for cultural heritage building classification using transfer learning and data augmentation. J. Cult. Herit. **74**, 214–224 (2025). https://doi.org/10.1016/j.culher.2025.06.010
5. Yiğit, A.Y., Uysal, M.: Automatic crack detection and structural inspection of cultural heritage buildings using UAV photogrammetry and digital twin technology. J. Build. Eng. **94**, 109952 (2024). https://doi.org/10.1016/j.jobe.2024.109952
6. Huang, W.-C., Luo, Y.-S., Liu, W.-C., Liu, H.-M.: Deep learning-based crack detection on cultural heritage surfaces. Appl. Sci. **15**, 7898 (2025). https://doi.org/10.3390/app15147898
7. Karimi, N., Mishra, M., Lourenço, P.B.: Automated surface crack detection in historical constructions with various materials using deep learning-based YOLO network. Int. J. Archit. Herit. **19**, 581–597 (2025). https://doi.org/10.1080/15583058.2024.2376177
8. Zhou, J., Lu, Y., Zheng, K., Smith, K., Wilder, C., Wang, S.: Design Identification of Curve Patterns on Cultural Heritage Objects: Combining Template Matching and CNN-based Re-Ranking, http://arxiv.org/abs/1805.06862, (2018). https://doi.org/10.48550/arXiv.1805.06862.
9. Aamir, S.M., Ma, H., Khan, M.A.A., Aaqib, M.: Real-Time Object Detection in Occluded Environment with Background Cluttering Effects Using Deep Learning, http://arxiv.org/abs/2401.00986, (2024). https://doi.org/10.48550/arXiv.2401.00986.
10. Padalkar, M.G., Beltrán-González, C., Bustreo, M., Del Bue, A., Murino, V.: A versatile crack inspection portable system based on classifier ensemble and controlled illumination. In: 2020 25th International Conference on Pattern Recognition (ICPR). pp. 4009–4016 (2021). doi:10.1109/ICPR48806.2021.9412039.
11. Li, G., Liu, Q., Ren, W., Qiao, W., Ma, B., Wan, J.: Automatic recognition and analysis system of asphalt pavement cracks using interleaved low-rank group convolution hybrid deep network and SegNet fusing dense condition random field. Measurement. **170**, 108693 (2021). https://doi.org/10.1016/j.measurement.2020.108693
12. Zou, Q., Zhang, Z., Li, Q., Qi, X., Wang, Q., Wang, S.: DeepCrack: learning hierarchical convolutional features for crack detection. IEEE Trans. Image Process. **28**, 1498–1512 (2019). https://doi.org/10.1109/TIP.2018.2878966
13. Nguyen, T.Q., Phan-Vu, P., Nguyen, P.T.: AI-based damage detection in prestressed concrete beams: a vision-integrated deep learning framework for crack localization and severity classification. Adv. Bridge Eng. **7**, 6 (2026). https://doi.org/10.1186/s43251-025-00194-0
14. Cha, Y., Choi, W., Büyüköztürk, O.: Deep learning-based crack damage detection using convolutional neural networks. Comput. Aided Civ. Inf. Eng. **32**, 361–378 (2017). https://doi.org/10.1111/mice.12263
15. Wei, J.: Based on an overview of crack detection. Sci. J. Technol. **6**, 133–137 (2024). https://doi.org/10.54691/dddp5674
16. Bochkovskiy, A., Wang, C.-Y., Liao, H.-Y.M.: YOLOv4: Optimal Speed and Accuracy of Object Detection, http://arxiv.org/abs/2004.10934, (2020). https://doi.org/10.48550/arXiv.2004.10934.
17. Zhang, K., Cheng, H.D., Zhang, B.: Unified approach to pavement crack and sealed crack detection using Preclassification based on transfer learning. J. Comput. Civ. Eng. **32**, 04018001 (2018). https://doi.org/10.1061/(ASCE)CP.1943-5487.0000736
18. Suryawanshi, V.D., Borse, D.I.S., Patil, D.R.V.: Deep learning-based crack detection in ancient paintings for digital art conservation. Open Access Int. J. Sci. Eng. **8** (2025)

19. Dwyer, B., Nelson, J., Hansen, T.: Roboflow [Software]. https://roboflow.com.
20. Jocher, G., Chaurasia, A., Qiu, J.: Ultralytics YOLOv8. https://github.com/ultralytics/ultralytics (2023)
21. OpenSistemas/YOLOv8-crack-seg. https://huggingface.co/OpenSistemas/YOLOv8-crack-seg.
22. Zde: File: Early Cycladic pottery, Mykonos, 2700–2300 BC, AM Mykonos, 224928.jpg. Wikimedia Commons Licensed under CC BY-SA 4.0. (2022). https://commons.wikimedia.org/wiki/File:Early_Cycladic_pottery,_Mykonos,_2700-2300_BC,_AM_Mykonos,_224928.jpg
23. Zde: File: Fruitstand, Neolithic pottery, Franchthi Cave, AM of Nafplio, 202057.jpg. Wikimedia Commons (2020). Licensed under CC BY-SA 4.0. https://commons.wikimedia.org/wiki/File:Fruitstand,_Neolithic_pottery,_Franchthi_Cave,_AM_of_Nafplio,_202057.jpg
24. Zde: File: Pottery kymbe painted ibexes 1700–1600 BC, PMTh 356 0503214.jpg. Wikimedia Commons (2014). Licensed under CC BY-SA 3.0. https://commons.wikimedia.org/wiki/File:Pottery_kymbe_painted_ibexes_1700-1600_BC,_PMTh_356_0503214.jpg